Tracking fluorescent and ferrimagnetic sediment tracers on an energetic ebb-tidal delta to monitor grain size-selective dispersal

Pearson, Stuart G.; van Prooijen, Bram; Poleykett, Jack; Wright, Matthew; Black, Kevin; Wang, Zheng Bing

DOI
10.1016/j.ocecoaman.2021.105835

Publication date
2021

Document Version
Final published version

Published in
Ocean & Coastal Management

Ocean and Coastal Management 212 (2021) 105835

Contents lists available at ScienceDirect

Ocean and Coastal Management

journal homepage: www.elsevier.com/locate/ocecoaman

Tracking fluorescent and ferrimagnetic sediment tracers on an energetic ebb-tidal delta to monitor grain size-selective dispersal

Stuart G. Pearson [a,b,*], Bram C. van Prooijen [a], Jack Poleykett [c], Matthew Wright [c], Kevin Black [c], Zheng Bing Wang [b,a]

[a] Faculty of Civil Engineering and Geosciences, Delft University of Technology, P.O. Box 5048, 2600 GA, Delft, the Netherlands
[b] Deltares, P.O. Box 177, 2600 MH, Delft, the Netherlands
[c] Partrac Ltd., Suite B3D, Milburn House, Dean Street, NE1 1LE, Newcastle-Upon-Tyne, United Kingdom

ARTICLE INFO

Keywords:
Sediment tracers nourishment sand transport

ABSTRACT

Sediment tracer studies use uniquely identifiable particles to track the pathways and fate of individual sand or silt grains in marine environments. These techniques are best applied to assess connectivity between potential sediment sources and sinks, such as between a sand nourishment and an ecologically sensitive area. Significant challenges exist when applying sediment tracing techniques to further understanding of systems with complicated hydrodynamic, sediment, and morphological regimes. Ebb-tidal deltas are highly dynamic coastal environments shaped by the complex interplay of waves and tides, but have been under-explored. In this study, we use dual signature (fluorescent and ferrimagnetic) sediment tracers to simulate the dispersal of dredged sediment placed as a sand nourishment on an energetic ebb-tidal delta (at Ameland Inlet, the Netherlands). After deployment, sediment dispersal and grain size sorting behaviour were monitored via the collection of seabed grab samples and magnetic sampling of sediment transported in suspension. The tracer content within collected samples were put in context with hydrodynamic conditions observed during the study period. Here we show that the use of such dual signature tracers, in addition to novel tracer recovery and analysis techniques, enables the dispersal of sediment to be monitored even in such complex settings and energetic conditions as an ebb-tidal delta. Our observations show that tracers transported in suspension are significantly finer than tracers that accumulated in the seabed. These suggest that preferential transport as a function of grain size is a key process in shaping the morphology of ebb-tidal deltas and thus governing the dispersal of sand nourishments there. The findings of this study and the approach used here provide valuable tools for assessing the baseline conditions of complex coastal environments today, and for planning the interventions which may be necessary in future responses to climate change. Lessons learned from the application of sediment tracers in this study are provided to assist future researchers and practitioners in applying this technique in dynamic coastal environments.

1. Introduction

Sand nourishments have proven to be an effective management strategy for reducing coastal erosion and are widely positioned as a means of coping with sea level rise (de Schipper et al., 2021; Lodder et al., 2019). While they are most common at beaches and foreshores (Hanley et al., 2014; Hanson et al., 2002; Liu et al., 2019; Stive et al., 2013), they are now also applied in other coastal settings like tidal flats (Baptist et al., 2019; van der Werf et al., 2019a).

Existing tools to predict and monitor the processes influencing the fate of a nourishment are however not yet sufficient. Seemingly trivial questions like: “Where, how much, when, and how to nourish?”, or “Where does the nourished sediment go?” are challenging to answer, but crucial for effective and efficient coastal management. This is especially the case for nourishments in complex settings like ebb-tidal deltas. Only a few examples of nourishments on ebb-tidal deltas are known (Bishop et al., 2006; Foster et al., 1994); on the contrary, ebb-tidal deltas have often historically been viewed instead as a source for nourishments (Fontolan et al., 2007; Hicks and Hume, 1997). However, nourishing ebb-tidal deltas is now being proposed as a key component of the Dutch coastal management strategy (Lodder et al., 2019; Wang et al., 2018). There is thus a pressing need to answer these basic questions.

* Corresponding author. Faculty of Civil Engineering and Geosciences, Delft University of Technology, P.O. Box 5048, 2600 GA, Delft, the Netherlands.
E-mail addresses: s.g.pearson@tudelft.nl, stuart.pearson@deltares.nl (S.G. Pearson).

https://doi.org/10.1016/j.ocecoaman.2021.105835
Received 15 April 2021; Received in revised form 9 July 2021; Accepted 18 July 2021
Available online 5 August 2021

A large-scale research program (KUSTGENESE2.0/SEAWAD) was initiated in the Netherlands to provide insights for designing nourishment on ebb-tidal deltas. The project included numerical modelling (Brakenhoff et al., 2020; De Wit et al., 2019; Reniers et al., 2019) and field measurement campaigns (van Prooijen et al., 2020; van der Werfet al., 2019b). Point measurements of hydrodynamics and suspended sediment characteristics were carried out at five locations across the delta. Bathymetric mapping provided snapshots of the ebb-tidal delta's morphological evolution in high spatial and temporal resolution (Elias et al., 2021). However, none of these methods tell us anything about the dispersal of sediment from a specific location, as in a nourishment. These methods also do not reveal sediment transport pathways, nor do they differentiate between pathways of different grain sizes. This type of information is necessary to predict the longevity of a nourishment, as well as its ecological impact.

Particle tracking or tracing is a method that can be used to obtain more insights into the pathways that sediment particles take. The former involves taking uniquely identifiable "tracer" particles, injecting a known quantity at a particular location, and then monitoring the dispersal of this tracer across space and through time (Black et al., 2007). This approach has been successfully employed to monitor nourishments by Smith et al. (2007). Unlike Eulerian measurements (at a fixed point in space), Lagrangian techniques like particle tracking can provide information about the fate and provenance of sediment. Most previous tracer studies have focused on using tracers to quantify transport rates and directions. For example, Ciavola et al. (1998), Oliveira et al. (2017), and Silva et al. (2007) used tracers to monitor alongshore transport rates. Komar (1978) and Wilson (2018) have used tracers to examine the relative degree of bed load and suspended load transport in coastal settings. By examining core samples of the seabed, Kraus (1985) and Sunamura and Kraus (1984) used tracers to monitor burial depths and quantify the mixing depth or "active layer" thickness.

Tracers can also be used to quantify grain size-dependent sediment transport and sorting processes. Allison et al. (2017) tracked the fate of tracer with multiple grain sizes, using differently-coloured tracers to represent different particle sizes. Robin et al. (2009) assumed that tracer particle size was uniform, and most previous studies focused only on matching the particle size distribution of the initial tracer to the native sediment, not how that distribution changes after being transported. A few studies have challenged this assumption and examined grain-size selective transport using tracers on straight, sandy beaches (Blackley and Heathershaw, 1982; Duane and James, 1980; Ribeiro et al., 2018). However, the potential of tracers to better understand sediment sorting and grain size-selective transport on ebb-tidal deltas is relatively under-explored, even though knowledge of such processes is essential to the design of effective nourishments there.

Execution of tracer studies in coastal settings is challenging due to the variety of physical processes influencing sediment transport and the numerous potential pathways that the tracer can take. Unlike in rivers where transport is driven mainly by unidirectional currents, the influence of waves or wind-induced currents must also be considered on open coasts (Hanes, 1988; Wilson, 2018). Even in relatively well-constrained coastal settings (e.g. straight, sandy beaches), there may be bidirectional tidal currents, stirring by waves, and wave-induced alongshore or cross-shore currents (Duane and James, 1980; Komar, 1978; Oliveira et al., 2017; Silva et al., 2007). Tracer studies have also been carried out at other coastal sites such as tidal flats (Kato et al., 2014), harbours (Khalfani and Boutiba, 2019; McComb and Black, 2005; Vila-Concejo et al., 2003), and navigation channels (Smith et al., 2007). The challenges of conducting and interpreting tracer studies are perhaps greatest in estuaries and tidal inlets, where complex interactions between waves, tides, and rivers may act in multiple directions.

Few studies have considered sediment tracers at coastal locations as dynamic and complex as tidal inlets (e.g. (Li et al., 2019; Moritz et al., 2011)). Most tracer studies conducted at tidal inlets have focused on intertidal shoals and beaches, where it is easier to deploy and sample the tracer material at low tide (Balouin et al., 2001; Oertel, 1972; Robin et al., 2009; Vila-Concejo et al., 2004). These studies were principally concerned with the migration of shoals and swash bars or sediment transport at the margins of the inlet. However, to the authors' knowledge, no tracer studies have considered transport on the distal lobe of an ebb-tidal delta. Sediment pathways here may be extremely convoluted and grain size-dependent (Elias et al., 2019; Herrling and Winter 2018; Pearson et al., 2020; Son et al., 2011), which greatly increases the uncertainty involved in designing a sampling plan to recover tracer placed there. Effectively monitoring the dispersal of sediment tracer on the outer limits of a highly energetic ebb-tidal delta at subtidal depths thus presents a daunting challenge and requires the use of new recovery and analysis techniques.

There are numerous techniques available to uniquely "tag" sediment to make it distinguishable from native background sediment. Natural geochemical properties of the sediment can be used (Clemens & Komar, 1988). Radioactive tracers were commonly used in the 1960s, but have since fallen out of favour due to their environmental impact (Courtois and Monaco, 1969; Duane and James, 1980; White, 1998). Radio frequency identification (RFID) tags can be used for larger gravel and cobble-sized particles (Miller and Warrick, 2012), although this approach is not feasible for sand-sized grains. Luminescence is also frequently used to trace sediment in geomorphological applications (Gray et al., 2019; Reimann et al., 2015). The most popular approach in recent years has been to apply a fluorescent coating to grains of sand, as the tracer can be identified visually or through automated image analysis (Gallaway et al., 2012; Komar, 1978; Kraus et al., 1982; McComb and Black, 2005; Miller and Warrick, 2012; Oliveira et al., 2017; Robin et al., 2009; Silva et al., 2007; Smith et al., 2007; Sunamura and Kraus, 1984). It may also be possible to trace particles via a comparative measure of the relative ease with which a material can acquire a magnetic field (i.e., the magnetic susceptibility of grains (Gallaway et al., 2012)). However, the risk of using tracer with a single unique identifying characteristic (termed a mono-signature tracer) is that it can limit the techniques which can be applied to sample tracer in the field and determine tracer content within samples in the laboratory. The solution to these issues may be the use of tracers that can be detected and distinguished via multiple properties.

In this paper, we explore the potential of particle tracking in energetic marine areas for monitoring the dispersal of nourishments. We aim to answer questions such as: "Is it possible to recover tracer particles in such dynamic environments?"; "What are efficient and effective ways to collect the particles?"; and finally: "What can we conclude from a particle tracking experiment that we cannot conclude from other monitoring techniques?". To simulate and predict the potential dispersal of sand from an ebb-tidal delta nourishment, we conducted a sediment tracer study at Ameland Inlet in 2017. Such a dynamic environment necessitated novel techniques for recovery and analysis of the tracer. A dual-signature (fluorescent and ferrimagnetic) tracer (manufactured by Partrac Ltd) was used, enabling samples to be collected from both the water column and seabed via a combination of suspended high-field magnets and seabed grab samples. Our approach afforded the opportunity to sample tracer deposited on the bed and transported as suspended load. The characteristics and location of recovered tracer provide useful information for understanding sediment sorting processes and differential transport as a function of grain size on ebb-tidal deltas from strategically placed sediment, as from a nourishment.

2. Background

2.1. Regional setting

Flood safety and vital ecosystems in the northern Netherlands depend on the fate of the Wadden Sea and Islands. Their morphodynamic response to sea level rise and sand nourishments is closely tied to the evolution of the ebb-tidal deltas between them. To understand the fate of these ebb-tidal deltas and effectively plan nourishments there, we must quantify the transport and dispersal of sediment as it moves across them.

The tracer study was conducted as part of a larger field measurement campaign which included simultaneous measurements of hydrodynamics, suspended sediment, bed sediment, seabed morphology, and benthic ecology across Ameland ebb-tidal delta, inlet, and Wadden Sea (Fig. 1). The location was chosen because it was the proposed site of a future sand nourishment project. Prior to this study in 2017, human interventions to the inlet had been relatively minor compared to other inlets on the Dutch coast (Elias et al., 2003; Wang et al., 2015). Ameland Inlet has been widely studied before (Cheung et al., 2007; Lenstra et al., 2019; van der Spek, 1996; Wang et al., 2016), and there are over 400 years of historical bathymetric data available (Elias et al., 2019). The abundance of both historic and present-day data makes Ameland Inlet the ideal location for such a study.

Historical bathymetry analysis by Elias et al. (2019) indicates that the recent evolution of Ameland ebb-tidal delta has been dominated by a pattern where the main ebb channel alternates positions and rotates in a clockwise direction. As the ebb-channel moves, shoals develop on the delta's periphery, and gradually move eastward where they eventually merge with the island of Ameland. The position of the ebb-tidal delta and main ebb-channel also determines the position of the eastern tip of the island of Terschelling. This morphodynamic evolution suggests the existence of eastward sediment transport pathways across the inlet and ebb-tidal delta. Mapping out these pathways and quantifying rates of sediment transport is essential to the design of nourishments on the ebb-tidal delta.

2.2. Hydrodynamic conditions

To provide context for the tracer measurements, we examine measurements of hydrodynamics and suspended matter carried out simultaneously during the deployment period. Van Prooijen et al. (2020) and van der Werf et al. (2019a) provide a general overview of the field campaign at Ameland Inlet, which took place over 41 days from August 29 to October 9, 2017. Henceforth, dates in this paper are given as $T+n$, where n is the number of days since the tracer release on August 29, 2017 (Section 3.2).

Water level, wave height, and near-bed current velocities were measured using a downward-facing high resolution Nortek Acoustic Doppler Current Profiler (ADCP-HR) mounted 0.50 m above the seabed (Nortek AS, 2008). From the wave characteristics and near-bed velocity, the maximum bed shear stress under combined wave and currents was computed using the method of Soulsby (1997). Changes in seabed level and acoustic backscatter were monitored using the altimeter on Nortek Acoustic Doppler Velocimeters (ADV) (Nortek AS, 2005) mounted 0.35 and 0.50 m above the bed. Together, these measurements provide additional information to assist in the interpretation of the observed behaviour of the tracer.

Hydrodynamic conditions at the outer lobe of the Ameland ebb-tidal delta during the measurement period were highly energetic, featuring

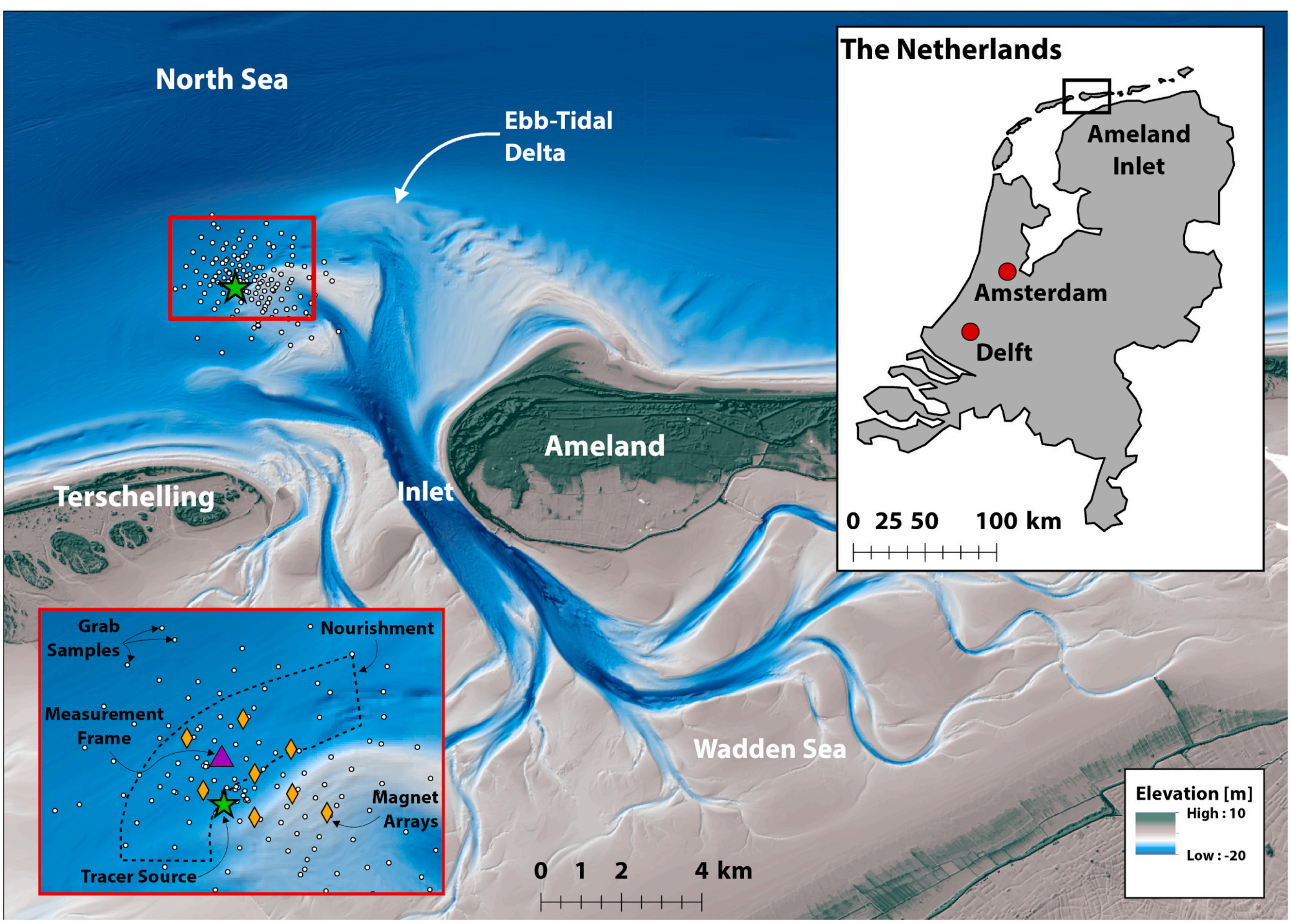

Fig. 1. Location of project site at Ameland Inlet, the Netherlands. The deployment site or source of the tracer is denoted by a green star. Orange diamonds indicate the location of suspended magnets, and yellow dots indicate seabed Van Veen grab sampling locations. The magenta triangle corresponds to Frame 4 of the Kustgenese2 measurement campaign (van Prooijen et al., 2020), with which measurements of hydrodynamic conditions were made during the field experiment.}. (For interpretation of the references to colour in this figure legend, the reader is referred to the Web version of this article.)

two major ($H_s > 4$ m) and three minor ($H_s > 1.5$ m) storms (Fig. 2b). The spring tidal range at the measurement frame is approximately 2.3 m, and current velocities can reach 0.5 m/s, predominantly flowing along an axis oriented east – west. The net displacement at the measurement frame was computed by integrating the measured velocities over time (Fig. 2f). These show a net eastward displacement from the vicinity of the tracer deployment site during the measurement period. In the 24 h after release, maximum tidal excursion from the measurement site is approximately 2 km westward and 4 km eastward (Fig. 2f). There is generally a strong eastward net displacement, with north or southward currents only dominating during the storms on T+15 and T+40 days.

Acoustic backscatter is frequently used as a proxy for suspended sand concentration (Green et al., 2000; van de Kreeke and Hibma, 2005). Although fine sediment is abundant in suspension on Ameland ebb-tidal delta, acoustic backscatter measurements here show stronger correspondence with sand (Pearson et al., 2021). The acoustic backscatter signal (measured with the ADV) shows clear semidiurnal peaks during ebb and flood currents, with higher peaks during flood and greater variability during spring tides. This corresponds to resuspension of local sand from the seabed. Relatively higher backscatter is also observed during the storms (e.g., T+16 and T+35 to 40).

Regular fluctuations of the seabed between August 31 (T+02) and September 5th (T+06) are on the order of 1–3 cm Fig. 2d, which matches the findings of Brakenhoff et al. (2020a,b), who found that wave-current ripples on Ameland ebb-tidal delta are consistently between 1 and 2 cm in height. The bed then continues to accrete episodically but erodes gradually during the intervening periods. The frame was repositioned following servicing on T+21, and the bed altimetry measurements become sparse thereafter. Caution should be taken when interpreting the bed levels after T+21.

These findings demonstrate that the seabed around the tracer deployment site is highly dynamic, even on the timescale of days to weeks. Combined with the energetic hydrodynamic conditions observed during the measurement period, there is strong potential for widespread tracer dispersal and/or burial.

3. Methods

To investigate sand transport processes on ebb-tidal deltas using sediment tracers, we broadly followed the methodological framework described by Black et al. (2017). This includes seven key steps:

1. Manufacture an appropriate tracer to match local sediment characteristics.
2. Perform a background survey of the site.
3. Release tracer in the field.
4. Recover tracer via sampling of the seabed and water column.
5. Separate tracer from background sediment in the laboratory.
6. Determine tracer content within samples.
7. Determine particle size of recovered tracer and background sediment.

3.1. Tracer preparation

A dual signature sediment tracer was manufactured by Partrac Ltd. for use in this study (Fig. 3). The coated mineral tracers have two signatures (fluorescent colour and ferrimagnetic character) applied as part of the coating process. These signatures are used to identify the particle unequivocally following introduction into the environment. In this study, each natural minerogenic kernel within the tracer batch was coated using a green fluorescent dye pigment with magnetic inclusions. The dye pigment is characterized by specific excitation and emission wavelengths, which facilitates a targeted sample analysis procedure. The tracer is consistently reactive upon exposure to ultraviolet (UV – A, ~400 nm) or blue light (~395 nm). The tracer grain will also adhere to any strong permanent or electro-magnet that comes into close proximity with it. This enables a simple separation of tracer within environmental (water, sediment) samples, a process which can also be exploited *in situ* through the use of submerged magnets (e.g., Guymer et al. (2010)).

A key requirement of tracer studies is that the tracer sediment needs to have similar physical and hydraulic properties to the native sediment it is intended to mimic (White, 1998), and that the properties of the tracer do not significantly change through time (Foster, 2000). This ensures that the tracer will be eroded, transported, and deposited in a similar manner to native sediments. A historic sample from the nearest available point to the proposed tracer release site served as a basis for the tracer (Rijkswaterstaat, 1999). Typically, differences of 10–15 % from the native grain size have been deemed acceptable in the peer-reviewed literature (Black et al., 2007; Robin et al., 2009; Vila-Concejo et al., 2004).

The sediment of Ameland ebb-tidal delta is largely composed of fine to medium sand (125–500 μm), grain size characteristics reflected by the available sample ($d_{50,native} = 271$ μm) (Fig. 4). Sediment composition on the nearby beaches of Ameland is approximately 84 % quartz, 10 % feldspar, 6 % heavy minerals, and has specific gravity (grain density) of $\rho_{s,\ native} = 2700$ kg/m^3 (Veenstra and Winkelmolen, 1976). An assessment of the physical and hydraulic equivalence between the manufactured sediment tracer and the native sediment on Ameland was performed. The tracer's physical characteristics ($d_{50,\ tracer} = 285$ μm, $\sigma_{1,\ tracer} = 0.48\ \Phi$, $\rho_{s,\ tracer} = 2628$ kg/m^3) closely matched those of the available pre-study native sediment sample ($d_{50,native} = 271$ μm) (Fig. 4). Approximately 60 % of the deployed tracer consisted of medium sand ($250 < d < 500$ μm), 35 % of fine sand ($125 < d < 250$ μm), and <5 % of very fine sand ($63 < d < 125$ μm). Although particles <63 μm were present in the deployed tracer, they are not considered for particle size analysis in this study, given the difficulty of optically identifying, counting, and sizing any recovered particles that small, and the project's overall focus on sand transport. Based on these data, it is reasonable to conclude that the manufactured tracer will form an effective tracer for use within the study.

3.2. Tracer release

To simulate the dispersal of sand as part of an ebb-tidal delta nourishment, tracer was released below the water surface and monitored across the period from August to October 2017. Immediately prior to the release of the tracer in August 2017, a background survey of the seabed sediment was carried out in the vicinity of the placement site to determine the presence and/or absence of particles with the same or similar characteristics as the tracer. Subsequent laboratory analysis revealed no presence of tracer-like fluorescent, magnetic particles in the bedded sediment prior to tracer deployment.

Based on the local grain size and typical local hydrodynamic conditions, it was expected that sand would be partly transported in suspension through the water column. To sample tracer particles travelling as suspended load, 8 arrays of suspended magnets were installed across the monitoring site in the hours before releasing the tracer (orange diamonds in Fig. 1). High field, Ne-Bn 11,000 Gauss bar magnets (30 cm in length and 2.5 cm in diameter) were covered in clear acrylic sheaths to facilitate the separation of recovered tracer from the magnet surface (e.g., Guymer et al. (2010)). These magnets were affixed to mooring lines at elevations of 1 m, 2 m, and 5 m above the seabed.

On August 29, 2017 (T+00), 2000 kg of tracer was released at 14:52 CEST on the northwest distal lobe of Ameland ebb-tidal delta (53.485° N, 5.5358° W, at the green star in Fig. 1) over a period of 14 min. A PVC pipe was affixed to the side of the ship (*MS Schuitengat*) and tracer poured down in buckets, with water sprayed down it to ensure continuous discharge and disaggregation of the tracer while in the release zone. The release technique was also intended to, as best as possible, mimic the placement of nourishment sand from a dredge hopper via a rapid release.

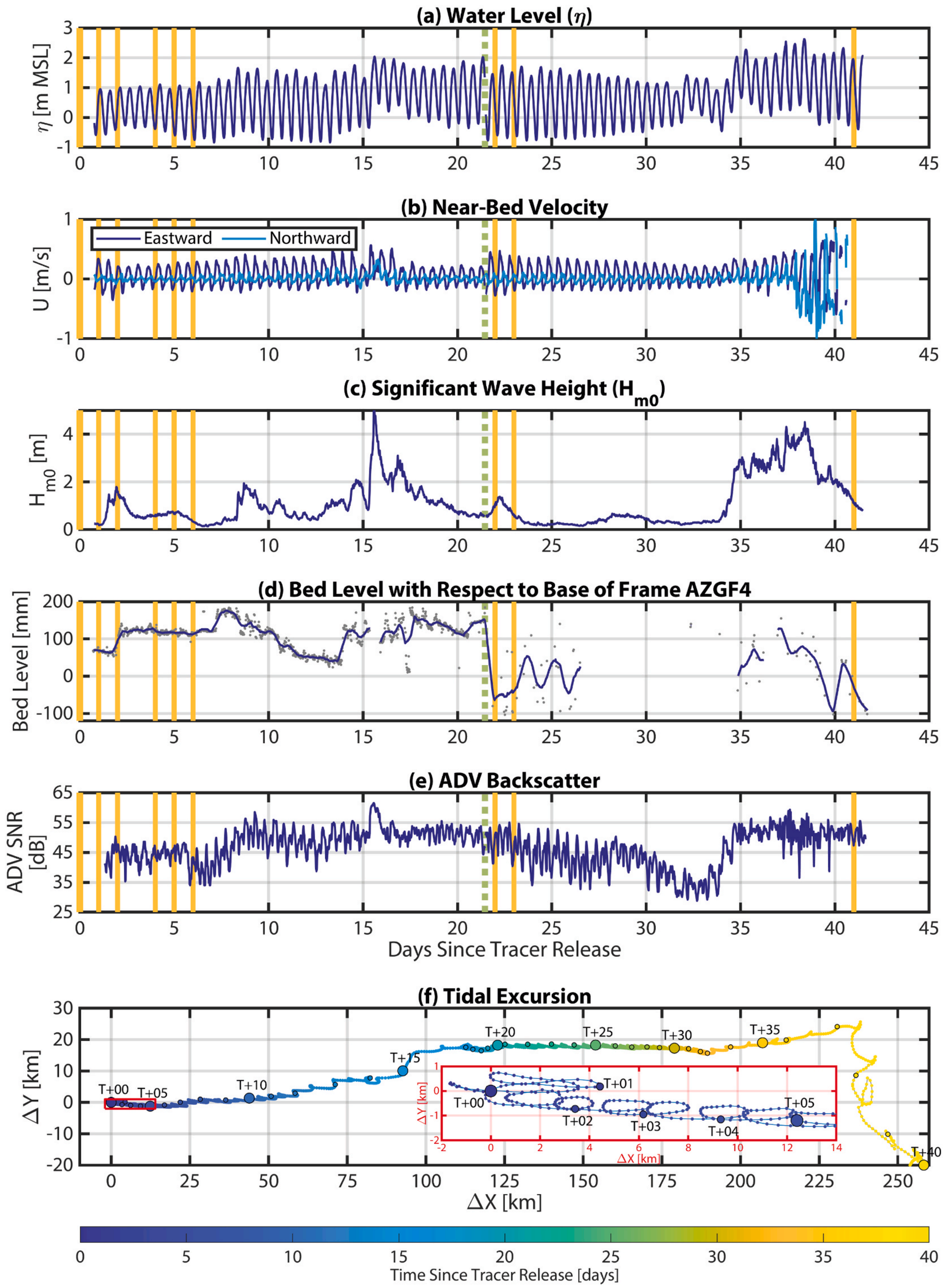

Fig. 2. Overview of hydrodynamic and seabed conditions measured near the tracer deployment site (AZG-F4) during the field campaign. (a) Water level with respect to mean sea level. Vertical yellow lines indicate days when tracer sampling occurred, and the green dashed line on day T+21 indicates when the frame was serviced. (b) Near-bed current velocity measured with a downward-facing ADCP-HR and averaged over a 0.5 m profile to the bed; (c) significant wave height (H_{m0}); (d) Bed level measured with ADV mounted 0.35 m above the bed. Note that position of frame shifts after being serviced on T+21, and bed level readings are sparse thereafter; (e) Acoustic backscatter measured using an ADV mounted at 0.5 m from the bed. Acoustic backscatter is given here as a proxy for suspended sediment concentration, with greater sensitivity to sand than fine sediment (Pearson et al., 2021); (f) Progressive vector diagram indicating total tidal excursion during the deployment period based on the near-bed current velocity measured by ADCP-HR during the 40-day deployment period. The red inset zooms in on the first 5 days (T+00 to T+05) after tracer release (August 29, 2017). Circles indicate the displacement at a given number of days after release, with larger markers indicating every fifth day. (For interpretation of the references to colour in this figure legend, the reader is referred to the Web version of this article.)

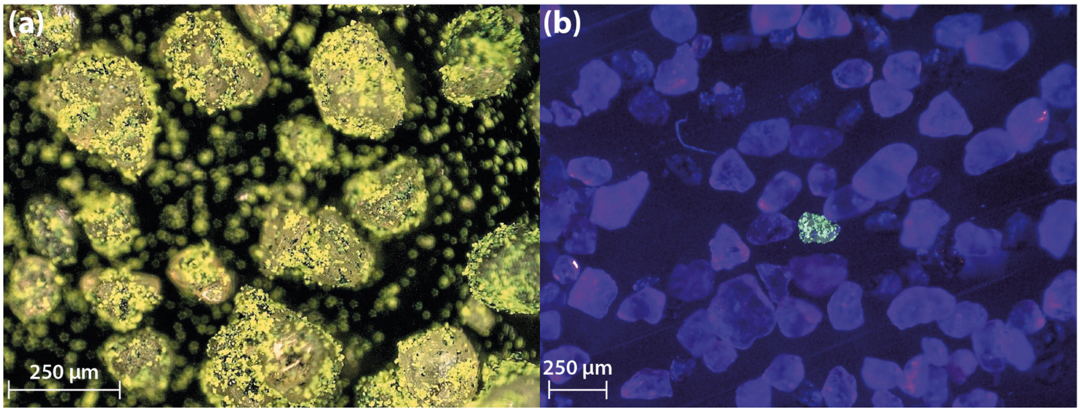

Fig. 3. (a) Tracer sediment particles with fluorescent and ferrimagnetic coating under normal lighting. (b) Seabed sample illuminated under 395 nm blue light. The fluorescent green tracer particles are unequivocally distinguishable from native sand grains and other types of particle in this lighting. Photos obtained using a Keyence VHX-5000 digital microscope (Keyence Corporation, 2014). (For interpretation of the references to colour in this figure legend, the reader is referred to the Web version of this article.)

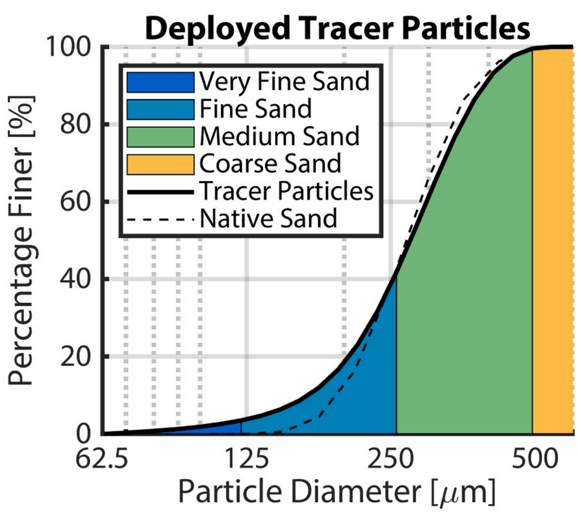

Fig. 4. Particle size distribution of deployed tracer sediment and native seabed sediment (from available pre-study data (Rijkswaterstaat, 1999)). Deployed tracer and native sediment largely consist of fine (125–250 μm) and medium (250–500 μm) sand.

Successful tracer studies require that the tracer is introduced to the target site with minimal loss and redistribution. The timing was selected to correspond with high water slack during a neap tide, which would minimize dispersal of the tracer by ambient currents before it reached the seabed. Offshore waves were small during the deployment procedure ($H_{s0} = 0.4$ m, $T_{m02} = 2.8$ s, $\theta = 270^\circ$), and thus offered fairly benign conditions for tracer settling. The depth of the water at the time and location of deployment was 6.9 m, which means that 95 % of the sand-sized tracer should have reached the bed within 11.2 min of deployment ($w_{s,d05=137\mu m} = 0.010$ m/s, based on (Soulsby, 1997)). Current velocity measurements did not begin until 2 h after the release (Fig. 2), but based on the drift of the ship (*MS Schuitengat*) during the release period (<100 m, Fig. 5a), currents were minimal.

3.3. Tracer recovery

The sampling scheme for recovering tracer was designed to maximize the chances of retrieving tracer particles in a dynamic environment where widespread dispersal was likely. Over the next 41 days, the spatiotemporal distribution of the tracer was monitored via the collection of 209 seabed grab samples. A sampling grid was initially defined in an approximately radial pattern surrounding the proposed tracer source site, with higher sampling density towards the point of tracer release and sparser coverage further away. The assessment of tidal excursion indicates that after 5 days, tracer grains mobilized under tidal flows could be dispersed on the order of 10 km away (Fig. 2f). This is beyond the bounds of the area within which it is practically possible to focus sampling resources (~3 km radius). If we assume that tracer with a d_{50} of 285 μm was uniformly distributed across this area, sufficient tracer was released $O(10^{10}$ grains) to ensure an average of 22 grains per grab sample. This suggests that a large enough quantity of tracer was placed to ensure a meaningful prospect of recovery. Due to several practical issues (discussed in Section 5), post-release sampling was limited.

Seabed samples were obtained from the *MS Siege* using a Van Veen grab to a maximum depth of 8 cm, with an average mass of 1.7 kg (n = 190). Once on deck, excess water was slowly drained from the grab sampler, and handheld blue flashlights (~395 nm) were used to assess the initial presence or absence of tracer particles. Grab samples were double-bagged in 2 L plastic bags, labelled, and stored in plastic crates out of direct sunlight.

Suspended magnets were recovered on August 30th (T+01) by the *MS Terschelling*, although adverse weather conditions meant that the recovery of two sets of magnets (K and L) was delayed until September 2nd (T+04). The 5 m magnet at location I was lost during recovery after it became attracted to the hull of the ship. Once lifted on deck, the magnets were removed from their mooring lines and visually inspected with blue light to determine the presence or absence of tracer. The plastic sheath was then carefully removed and its contents washed through a funnel into a 1 L sampling jar. Magnet samples typically weighed 0.1–1 g (n = 21), but sample masses between 16 and 27 g were obtained in three cases. All sampling equipment was carefully washed between samples to reduce the risk of cross-contamination between samples.

3.4. Quantifying tracer content within environmental samples

To quantify the tracer content (particle counts) within environmental samples, each sample was first processed. Each sample was dried in an oven at 180 °C until no further change in mass was observed. The material was smoothed to an approximately granular monolayer on a large black board, and then a preliminary visual inspection for tracer particles was performed using a handheld blue light (~395 nm). Samples revealing fluorescent particles were then magnetically screened to further distinguish tracers from other fluorescent matter (i.e., microplastics, which were commonly observed). A permanent, high field Ne-Bn 11,000 Gauss magnet was then passed across the sample at a distance

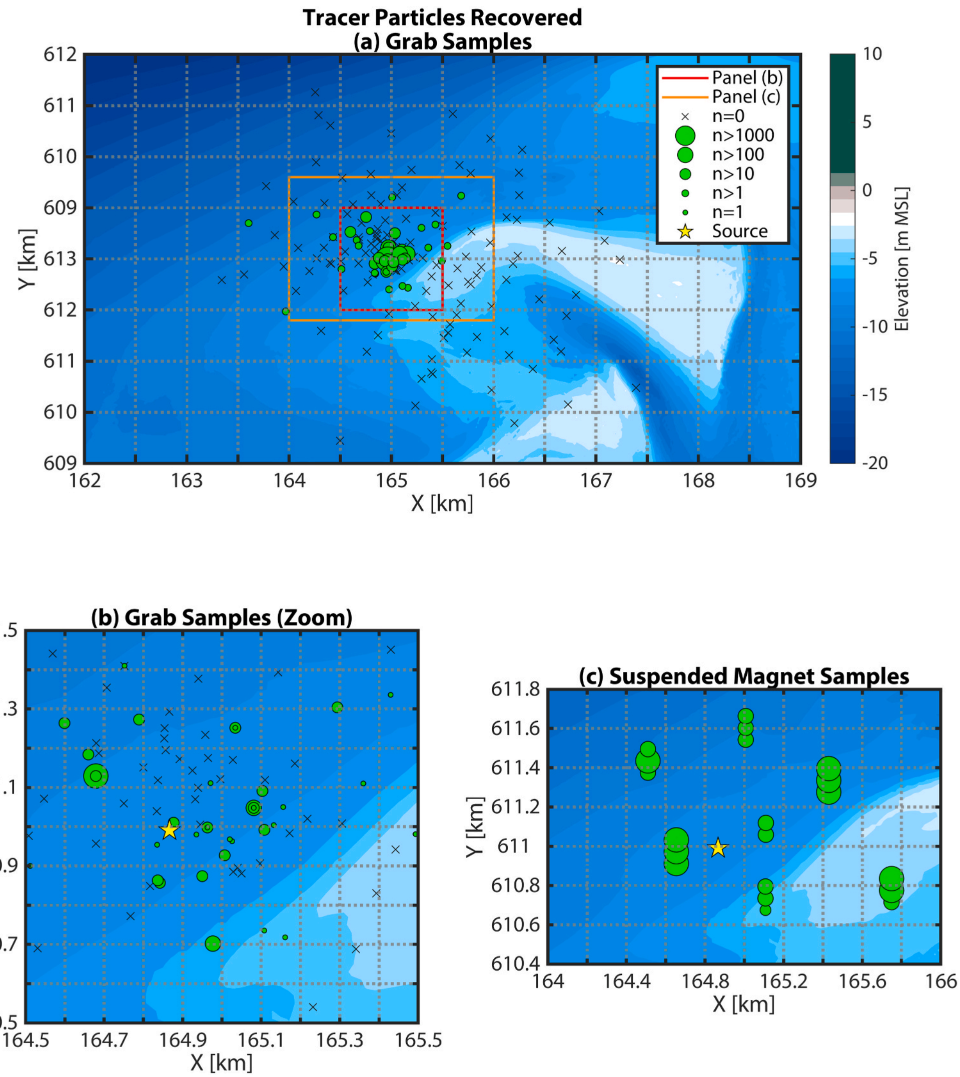

Fig. 5. Spatial distribution of tracer recovered in the first 41 days after deployment, indicating the number of tracer grains recovered from each sample. (a) Tracer samples obtained via seabed grab samples. (b) Tracer samples obtained via seabed grab samples, zoomed in on central area with denser sampling. (c) Samples obtained using suspended magnets. The tracer release location is indicated by a yellow star. X-symbols indicate samples in which no tracer particles were found. (For interpretation of the references to colour in this figure legend, the reader is referred to the Web version of this article.)

of 2–3 mm, facilitating separation of magnetic particles, or sifted through the sample where samples were larger. This procedure was repeated, with intermittent cleaning and recovery of the particles from the surface of the magnet, until no further magnetic particles were extracted and no further fluorescent particles were found within the sample.

Once separated, the number of tracer gains were counted by eye; the error from visual counting should be below 5–10 % (Carrasco et al., 2013). To do this, the samples were systematically scanned with the aid of a hand tally counter. Where high tracer counts were observed, the sample was sub-sampled and the data extrapolated.

3.5. Particle size analysis

To investigate sorting behaviour of the tracer material as it dispersed in the environment, we measured the particle size distributions of the recovered tracer and native background sediment. Magnetically-separated samples containing visible tracer particles were examined using a Keyence VHX-5000 digital microscope (Keyence Corporation, 2014). Whilst illuminating the sample using blue light (~395 nm), high resolution photographs at 40-100x magnification were captured and stitched together into a mosaic of the entire sample. The microscope's automated image processing tools were used to obtain the equivalent circular diameter of each tracer particle in the sample (similarly to (Ribeiro et al., 2018)). Each grain was visually checked to ensure that the particles were accurately identified. Under 100x magnification, the bright green tracer particles were unequivocally distinguishable from native sand grains and other types of particle (Fig. 3b). Where there was a discrepancy in tracer count from the visual analysis, the count obtained via microscope prevailed. After each analysis, the sample was shaken to redistribute the position of the grains, and the procedure repeated to reduce potential biases in the image analysis.

The particle size distributions of native non-tracer sediment separated from the tracer samples were measured using a Malvern Mastersizer 3000 (Malvern Instruments Limited, 2017). At least 4 measurements were made per sample and then averaged together to provide a representative distribution.

4. Results

Tracer particles were recovered from 45 of 190 seabed grab samples (24 %) and 24 of 24 magnetic samples (100 %), despite the occurrence of conditions capable of mobilizing 99 % of the deployed particles (Fig. 10). Although hydrodynamic measurements indicate an eastward tidal residual flow (Fig. 2f), the spatial pattern of the recovered tracer indicates that transport dispersed the tracer in all directions relative to the release site, likely due to a combination of tidally driven transport and wave action.

Tracer material was recovered from the grab samples taken in the first week after deployment, up to 1325 m away from the source (Fig. 5).

Although the majority of samples are clustered within 500 m of the release site, there is no distinct trend in their spatial distribution. Most of these samples were recovered between August 30th (T+01) and September 4th (T+06), but some tracer was even recovered from the tracer source on October 9th (T+41), after two large storms had passed. In total, 14 of the tracer samples contained a single tracer particle, 13 had 2-10 particles, 14 had 11-100 particles, 14 had 101-1000 particles, and 11 samples contained more than 1000 particles. All but one of the latter were obtained via suspended magnets.

The tracer particles recovered from the seabed (mean d_{50} = 212.8 μm, σ_{d50} = 74.3 μm, σ_1 = 0.48 Φ) were finer and better sorted on average than the original tracer (d_{50} = 274.4 μm, σ_1 = 0.34 Φ) (Fig. 6). The samples recovered by the magnets (mean d_{50} = 81.9 μm, σ_{d50} = 6.0 μm) are significantly finer than both the original tracer sample and the samples recovered from the bed (Fig. 6).

On average, tracer particles are largest closer to the bed (d_{50} = 83.9 μm at 1 m above the bed), decreasing slightly with elevation (d_{50} = 80.6 μm at 2 m above the bed) (Fig. 7). The particle size is negligibly different at 5 m above the bed (d_{50} = 81.0 μm). All suspended samples are well sorted (σ_1 < 0.5 Φ) based on Folk & Ward Logarithmic Graphical measures (Blott and Pye, 2001), where increased sorting corresponds to reduced spread around the mean particle size. Sorting is poorest at 1 m above the bed (σ_1 = 0.41), but improves slightly at 2 m and 5 m above the bed (σ_1 = 0.38 Φ and σ_1 = 0.39 Φ, respectively).

Although there is a marked difference between the original tracer and the material recovered in the water column, the particle size distributions of suspended tracer samples do not vary substantially with elevation from the bed. This is consistent with Beamsley et al. (2001), who observed that although median particle size decreases with height above the bed, the modal peak of suspended sand grain size distributions stays relatively consistent. They attribute upward fining to an inverse relationship between concentration profile gradient and grain size, with finer particles being more dominant at higher elevations.

The particle size distribution of recovered tracer particles can also be considered spatially (Fig. 8). Among samples with more than one grain (it is not meaningful to compute d_{50} and sorting from a single particle), there is a weak negative correlation between median grain size (R^2 = 0.224) and increasing distance from the source (Fig. 9). Furthermore, the mean d_{50} of the magnet samples is < 100 μm, with all seabed samples consistently coarser. The envelope of grain size variability shrinks with distance from the source: the variation in d_{50} decreases further away. A very weak negative correlation is observed between sediment sorting coefficients of multi-grain samples and distance from the source

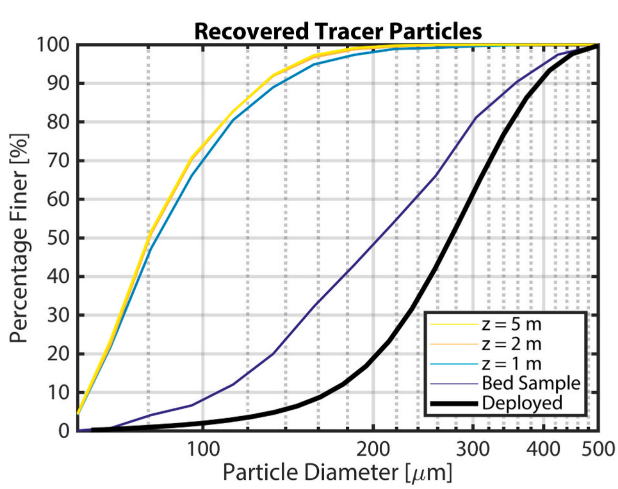

Fig. 6. Mean particle size distributions of tracer recovered from the seabed and suspended magnets at z = 1, 2, 5 m above the seabed. Magnetically-recovered tracers were significantly finer than those acquired via grab sample from the seabed.

(R^2 = 0.082), which implies that the tracer become slightly better sorted with distance. These patterns are consistent with the frequently-observed trend of fining and better sorting along transport pathways in complex marine environments (Le Roux and Rojas, 2007; Poizot et al., 2008).

To better visualize the influence of the hydrodynamic conditions on the potential transport modes of tracer particles and explain the observed differential transport, we computed the inverse Rouse number ($\kappa u^*/w_s$) of four grain size classes using the method of Soulsby (1997) (Fig. 10). The medium sand (250–500 μm) comprising most of the tracer travels mainly as bed load, only moving into suspension during the two largest storms (September 13 & October 3). This could explain its absence on the suspended magnets, which were all collected by September 2. Fine sand (125–250 μm) travels in suspension during minor storms and also at spring tide, whereas very fine sand grains (63–125 μm) are nearly always travelling as suspended load.

These estimates are consistent with existing numerical model simulations of Ameland Inlet (Reniers et al., 2019). Modelled daily averaged sediment transport of 200 μm sand near the tracer deployment site is principally tidal suspended transport in calm conditions, whereas suspended transport due to wave skewness dominates during storms. Huisman et al. (2016) found that grain size-selective sediment transport at a sand nourishment on the Dutch coast was most prevalent during mild and moderate conditions when some but not all of the bed material is mobilized. Finer sand classes will thus be entrained more frequently into the water column (Fig. 10). In more intense conditions, sorting behavior is still present but to a lesser degree, since all size classes are mobilized, including coarser particles. However, it is mild and moderate conditions that prevail during the first 6 days of tracer sampling.

We can quantify the potential impact of a nourishment on the native grain size distribution by analogy using recovered tracers. We compared the grain size characteristics of each tracer sample with the native sediment that it was recovered in. The native background sediment samples containing tracer are overwhelmingly homogeneous, well-sorted fine (F) sand, with a mean d_{50} of 200.2 μm (σ_{d50} = 21.7 μm), and mean sorting coefficient of 0.50 Φ (Fig. 11). Conversely, the recovered tracer shows a wide variation in d_{50} from 100 to 400 μm (mean d_{50} of 212.8 μm, σ_{d50} = 74.3 μm), and is on average 12.6 μm coarser than the native sediment in which it was recovered. The recovered tracer is negligibly better-sorted on average, but shows more variation in sorting than the native sediment. Comparing the particle size analysis of recovered tracer and the native sediment in which it was found reveals clear signs of grain size-selective transport.

5. Discussion

We recovered tracer sediment on a highly dynamic ebb-tidal delta as part of a study to understand the potential spreading of nourishments there. The high recovery rates of tracer on an energetic subtidal ebb-tidal delta in spite of sampling limitations are a proof of concept for using tracers to monitor sediment dispersal in such environments. In particular, the suspended magnets were revealed to be an effective means of capturing tracer particles suspended throughout the water column. Furthermore, microscopy analysis enabled the determination of different grain sizes within the collected samples, facilitating the assessment of differential transport (per grain size) following tracer release.

Grain size influences both the persistence and ecological impact of sand nourishments. Nourished sand will tend to disperse more quickly if its grain size is smaller than native sediment, which thus determines how long it will persist at its placement site (Dean, 2002). As such, grain size of placed material relative to native sediment is often a key parameter in nourishment design (Hanson et al., 2002). Grain size also influences benthic habitat (McLachlan, 1996), and the recovery of benthic ecosystems after a nourishment can be impeded if nourished sand grain characteristics do not closely match the native sediment (Bishop et al.,

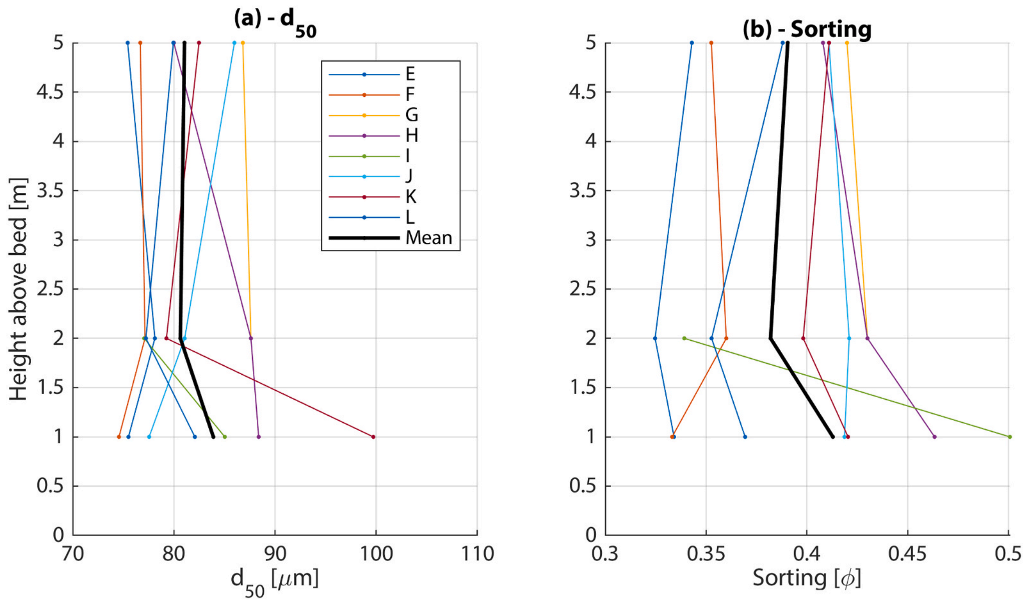

Fig. 7. Particle size statistics of tracer recovered from the seabed and suspended magnets at z = 1, 2, 5 m above the bed. (a) Median particle diameter (d_{50}); (b) Sorting. Thin lines correspond to individual magnet locations, and thick black lines are averaged across all samples.

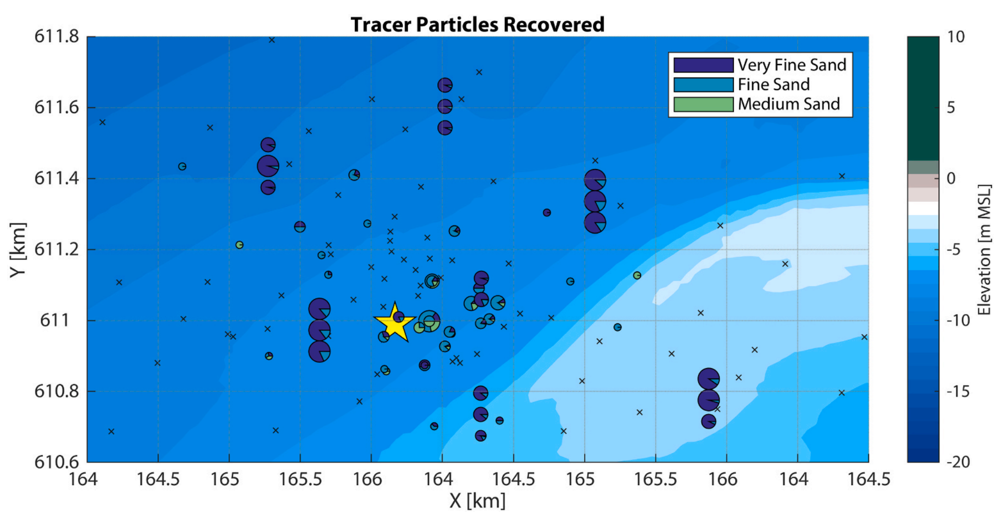

Fig. 8. Spatial distribution of tracer with pie charts indicating the relative fraction of a particular sediment class. The size of the pie chart is proportional to the number of particles found in a given sample. X-symbols denote samples in which no tracer particles were found.

2006; Defeo et al., 2009; Peterson et al., 2014). Tracer particle size analysis like that carried out in this study is thus a useful technique for understanding the grain size-specific evolution of nourishments. By releasing tracers in conjunction with nourishments (e.g., Smith et al. (2007)) and then tracking tracer particle size, coastal managers can improve the efficacy of nourishments and monitor potentially negative ecological impacts.

Our study's findings are summarized in a conceptual diagram (Fig. 12). Finer grains become preferentially resuspended and transported further than coarser grains. The coarser grains are mobilized less frequently and travel more as bedload, which leaves them more susceptible to burial (e.g. Fig. 2d) or integration into bedforms. Material travelling in suspension travels more quickly than material moving as bedload, so finer tracer particles are also found further from the source. Superdiffusive behaviour due to correlated grain motion and grain size heterogeneity may explain the solitary coarser grains of sand found farthest away from the source (Martin et al., 2012).

Two days after the tracer release (T+02), the bed accretes by approximately 8.5 cm in 7 h, mostly during flood tide following the peak of a small storm (Fig. 2d). It is therefore possible that tracer particles deposited on the seabed within this area could have been buried beyond the reach of the Van Veen grab sampler used to extract the sediment (approximately 8 cm). This is consistent with the historical bathymetry analysis of Elias et al. (2019) and Elias et al. (2021), which shows this region of the ebb-tidal shoal to be prograding and hence depositional. Sampling via deeper cores may yield greater insight into the burial of tracers and sediment balance in future studies.

The tracer dispersal pattern in Fig. 8 does not appear to coincide with the eastward direction of net tidal excursion (Fig. 2f). This may be explained by the difference between residual (net) transport and gross transport. If the tidal flow is bi-directional, the residual is a small difference between the much larger gross flood and ebb transports. In open water, sediment transport vectors form an open ellipse over the course of a tidal cycle, just like the flow velocity vectors. Where the tracer can be found back is not determined by the residual transport field, but by the gross transport field, which is highly variable in direction during a tidal

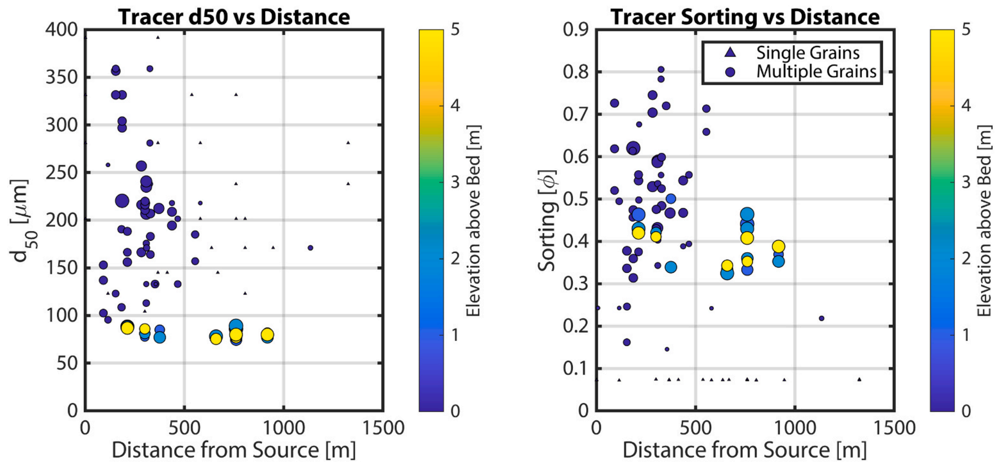

Fig. 9. Comparison showing distance from the tracer source vs (a) d_{50} and (b) sorting of recovered tracer. Triangular markers indicate single grains, whereas circles indicate samples with multiple grains. The size of the symbol is proportional to the number of particles found in a given sample. The colour of the markers indicates sample elevation above the bed. (For interpretation of the references to colour in this figure legend, the reader is referred to the Web version of this article.)

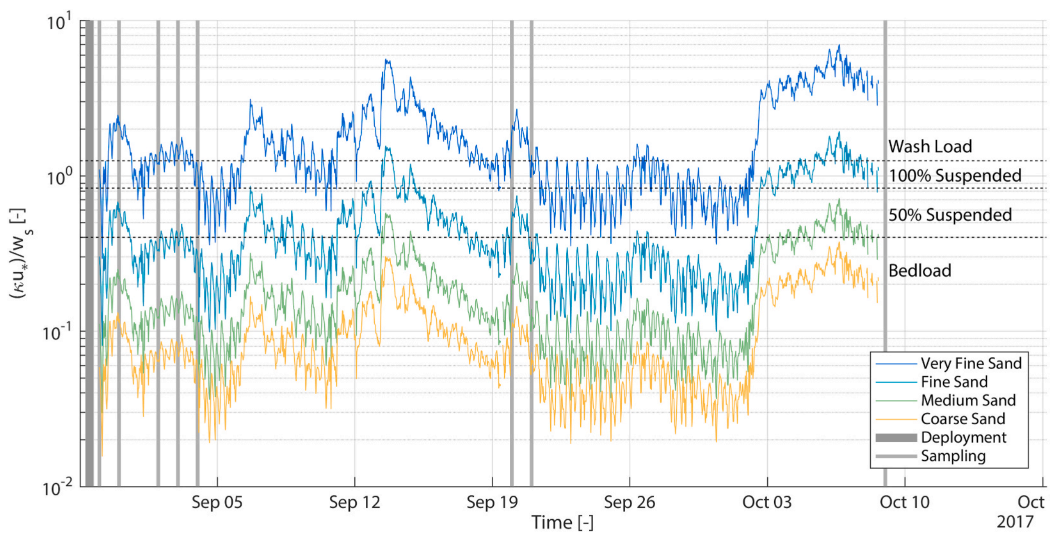

Fig. 10. Inverse Rouse number ($\kappa u^*/w_s$) and transport mode for each sediment class. Calculated using the method of Soulsby (1997) from wave and near-bed velocity measurements taken by a downward-facing ADCP-HR near the tracer source (mounted 0.5 m above the seabed). Tracer sampling dates are indicated by grey bars.

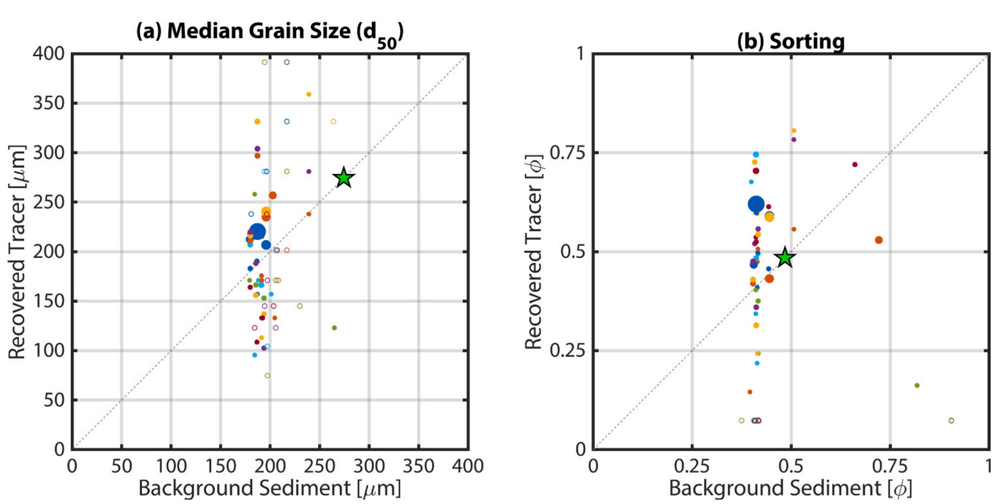

Fig. 11. Particle size statistics of native background sediment vs recovered tracer. (a) Median particle size (d_{50}), (b) sorting coefficient. Hollow circles represent samples with only single tracer grains, and solid circles represent samples with multiple tracer grains. The size of the circles is proportional to the number of tracer grains found in the sample. The green star indicates the properties of the tracer that was initially released. (For interpretation of the references to colour in this figure legend, the reader is referred to the Web version of this article.)

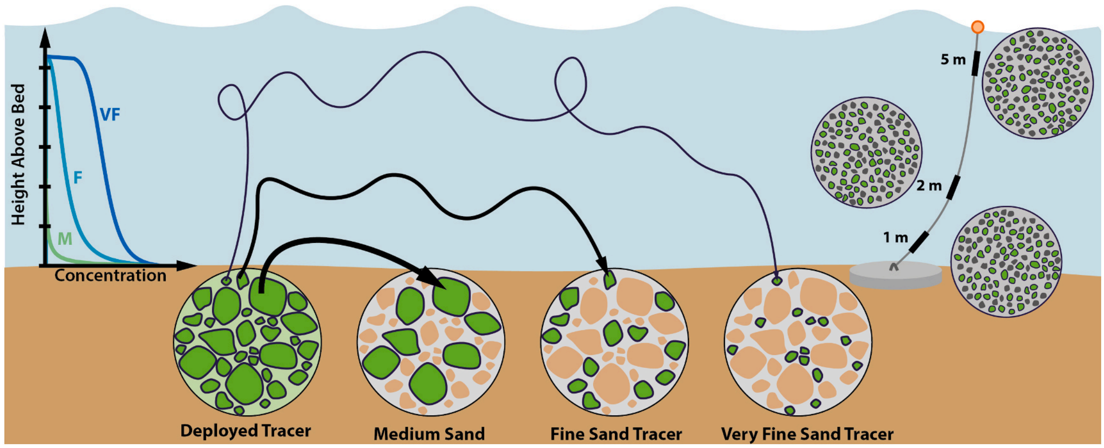

Fig. 12. Conceptual diagram indicating dispersal of tracer on the seabed and in the water column. Finer grains are preferentially resuspended and transported further than coarser grains, which travel more often as bedload and are more susceptible to burial. Suspended sand grains observed on the magnets were overwhelmingly very fine, with little difference as a function of height above the bed.

cycle. This may be evidence of chaotic stirring, which is known to occur at tidal inlets similar to Ameland (Ridderinkhof and Zimmerman, 1992). Ridderinkhof & Zimmerman showed that after just a few tidal cycles, particles can be dispersed in highly spatially heterogeneous patterns that do not necessarily coincide with the direction of net transport. This hypothesis could be tested via Lagrangian sediment particle modelling (e.g., Soulsby et al. (2011)).

One of the key findings of this study was the effectiveness of magnets mounted on mooring lines through the water column at capturing suspended tracer particles. The magnets in this study typically recovered several orders of magnitude more tracer particles than grab samples taken from the seabed. Tracer particles found in grab samples were deposited on the seabed, and hence give an indication of sediment accumulation there. However, tracer recovered by the suspended magnets is indicative of grains that are actively moving as suspended load. Very fine grains of tracer (63–125 μm) made up a small fraction of the tracer particles recovered in the bed but were abundant on the suspended magnets. This supports the expected theory that sorting due to differential suspended transport by grain size is a key process on the ebb tidal delta.

Although tracer studies are a well-established tool in the arsenal of coastal scientists and engineers, challenges associated with their deployment have typically limited their application to more well-constrained settings like alongshore uniform beaches. Previous applications to tidal inlets and ebb-tidal deltas have tended to focus more on intertidal areas which could be more easily sampled, whereas this study investigates a fully subtidal site. In this study we also successfully employ innovative methods for both recovery (e.g., suspended magnets) and analysis (e.g. particle size analysis of recovered tracer via microscopy) in a very dynamic setting, demonstrating that these techniques can be used in such environments. However, the purpose and method of application must be carefully considered in study planning. These advances expand the range of environments in which tracer studies can be conducted, but also increase the amount of data that can be gained from such a study. Since tracer studies can be labour-intensive, time-consuming, and challenging to execute (Ciavola and Grottoli, 2017; White, 1998), it is important to find new ways to add value to them, both in terms of practicalities but also in terms of expanding their scientific worth. The following section provides lessons learned from the study, which we hope will be useful for future researchers/practitioners interested in utilizing sediment tracers in highly dynamic environments:

- Dual tracer signatures (fluorescence and ferrimagnetism) were very beneficial, increasing the ease of tracer recovery in the field and analysis in the laboratory. In particular the suspended magnets placed on mooring lines were both an effective means of recovering tracer and potentially offer a route to sampling the suspended sediment load in deeper water or environments where it is challenging to sample frequently, but also an afforded an "opportunistic" measurement: the magnets were place on marker buoys of pressure sensors mounted on the seabed as part of a different experiment (De Wit et al., 2019; Reniers et al., 2019).
- Magnets were highly effective at recovering tracer, with large quantities of tracer particles (>1000) found on all of the recovered magnets. In addition, magnetic non-tracer particles were found within the seabed grab samples and especially attached to the suspended magnets. The high recovery rates of tracer from the magnets indicates that some of the tracer particles travelled in suspension, for at least part of the measurement period. It is unlikely that the sediment captured by the magnets is from the initial tracer release, given that deployment took place at high water slack, and that deposition of all sand-sized tracer would have occurred within half an hour. This is especially true for magnets located east (upstream) of the ebb currents that followed release (i.e. Fig. 2f). Tracer recovered on the magnets is thus likely indicative of resuspended sand.
- The use of a digital microscope expanded our tracer analysis capabilities significantly beyond what is possible with only the naked eye. The microscope allows for unequivocal identification of tracer particles, automated particle enumeration, and estimation of tracer particle size distributions. This reduces the likelihood of human error in tracer particle characterization and enables topics such as sediment sorting to be investigated. Robin et al. (2009) assumed that the grain size distribution of the tracer is identical throughout the entire plume. However, the spatial variations in particle size relative to the original tracer particles observed in this study challenge this assumption. Future tracer studies should thus consider microscopy analysis to investigate grain size characteristics.
- The primary study limitation was our inability to perform frequent, spatially repeated sampling due to challenging sea conditions and practical issues such as vessel availability. Sampling resources prioritized maximum potential recovery of tracer within the available ship time, rather than keeping a regular sample grid in space and time. Further possibilities for tracer sampling were eliminated by the placement of a 5 Mm^3 sand nourishment directly on top of the tracer

release site beginning in March 2018. Collectively, these conditions led to a disparate sampling campaign which prevented the meaningful derivation of general spatial statistics (e.g. tracer plume centroid movement in time and space), and application of the spatial integration method (e.g. (Robin et al., 2009; Vila-Concejo et al., 2004; White, 1998)) to account for the dispersed tracer mass. This kind of analysis is achievable on a beach face, for example, but on a highly dynamic ebb-tidal delta spanning several kilometers in size, the extrapolation of particle counts may be dubious.
- Tracer studies with similar logistical constraints should prioritize consistent sampling at fewer sites over attaining wider spatial coverage with limited repetition in time. It is essential to clearly identify the purpose of deploying sediment tracers, so that a considered, targeted and achievable, sampling plan can be developed and implemented. When working in an open system where significant dispersion is likely, it is necessary to focus sampling resources on tracer recovery and balance that against the goals of the project. In highly dynamic environments, the use of tracers to monitor sediment transport pathways over extended temporal periods is not advised. Careful consideration of site data prior to tracer deployment to determine the best positions for release and sampling is essential.
- The sample selected from Rijkswaterstaat (1999) to serve as a model for the tracer particle size distribution was coarser ($d50 = 270.7$ μm) than most of the native sediment samples obtained during the tracer study (mean $d50 = 200.2$ μm) (Fig. 11). Even though the tracer closely matched the target sample, that sample was not very representative of the present-day conditions on that part of the ebb-tidal delta, likely due to the shifting position of channels and shoals (e.g., Elias et al. (2019)). This shows the importance of using recent reference sediment samples for tracer studies in such dynamic areas. However, this problem was circumvented by performing optical grain size analysis on the recovered tracer, which permitted analysis of tracer particles that were closer in size to the native sediment. In addition, the relative absence of recovered medium tracer compared with the amount that was initially placed strengthens the case for differential transport as a key mechanism.

This study also provides guidance for carrying out nourishments on ebb-tidal deltas in the future. The behaviour observed in this field experiment suggests that fine nourishment sand applied to Ameland ebb-tidal delta will also be highly dispersive, which may be important for estimating the lifetime and ecological impact of a nourishment. Tracer studies do not account for indirect effects of the nourishment on sediment transport (e.g. due to modification of local flow and transport fields), but they do enable unequivocal identification of sediment from a particular source. Thus, a useful application of tracers for nourishment design and monitoring would be to combine the tracers with the nourished sediment as it was placed, similarly to Smith et al. (2007). In this way, the performance of the nourishment could be monitored using conventional bathymetric surveys, but it would also be possible to differentiate nourished sediment from native sediment using tracer as a proxy. If the goal of a tracer study is to establish whether particles from a given source (e.g., nourishment) reach a given location (e.g., an ecologically-sensitive area), then the target site could be surrounded by suspended magnets as a means of intercepting tracer. This would give an indication of the quantity and characteristics of nourished sediment reaching the target site.

The results obtained in this study also fill a need for high-quality data to further validate models of grain size-specific transport of nourished sediment (de Schipper et al., 2021), particularly Lagrangian models (MacDonald and Davies, 2007; Soulsby et al., 2011). These models can be used to predict the pathways, receptors, and system-wide connectivity of nourished sediment (Pearson et al., 2020), providing coastal researchers and managers with additional tools for analysis and design.

6. Conclusions

In this study, we presented the results of a sediment tracer study carried out on the energetic ebb-tidal delta of Ameland Inlet in the Netherlands. We aimed to answer the questions: “Is it possible to recover tracer particles in such dynamic environments?”; “What are efficient and effective techniques to collect the particles?”; and finally: “What can we conclude from a particle tracking experiment that we cannot conclude from other monitoring techniques?”

The use of a dual-signature tracer (fluorescent and magnetic) aided both recovery in the field and analysis in the laboratory. Despite the very energetic and open environment, we found tracer particles in 45 of 190 grab samples (24 %) and on 24 of 24 suspended magnets (100 %). Generally, only small numbers of particles (O(1–100)) were found using grab samples. The suspended magnets provided a much more effective tracer recovery technique than the seabed grab samples: O (1000–10000) particles were retrieved in this manner. The higher efficiency of suspended magnets boosts the chances of tracer recovery and could lead to cost savings by requiring less tracer sediment to be deployed or fewer seabed grab samples. Furthermore, the application of suspended magnets for recovering tracer opens new possibilities for measuring sediment pathways, as it is an indication of the sediment in suspended transport, instead of an indication of sediment deposition (as measured by grab sampling). Analysis of tracer particle size via digital microscopy enabled additional data to be extracted from the recovered tracer than merely counting the amount observed within the sample.

The methodology in this study expands the range of environments in which tracer studies can be completed by demonstrating successful tracer recovery in a setting characterized by dramatic morphodynamic changes and convoluted sediment transport pathways. In doing so, we increase the potential knowledge yield that can be gained from such field experiments. We also offer a series of lessons learned and recommendations for the use of sediment tracers in highly dynamic environments to support future research and coastal management practice. Particle tracking is the only technique that can directly measure the provenance of sediment, but its full potential is seldom realized due to common challenges in recovery and analysis. The techniques explored here (e.g., magnetic tracer retrieval and separation, microscopic analysis of tracer) provide additional means of generating value from tracer studies. These approaches increase our ability to tap into the unique perspective on sediment transport that tracers offer.

Declaration of competing interest

The authors declare that they have no known competing financial interests or personal relationships that could have appeared to influence the work reported in this paper.

Acknowledgements

This work is part of the research programme ‘Collaboration Program Water’ with project number 14489 (SEAWAD), which is (partly) financed by NWO Domain Applied and Engineering Sciences. Special thanks to the Dutch Ministry of Infrastructure and Water Management (Rijkswaterstaat and Rijksrederij) for organizing the field campaign and for their ongoing support as part of the Kustgenese2.0 project. Thanks also to the crew of the *MS Schuitengat, MS Siege, and MS Terschelling* for their assistance with the fieldwork. Thank you to Claire Chassagne, Mohammed Jafar, and Saskia Huisman for their help with the laboratory equipment. Data from the 2017 Kustgenese2.0/SEAWAD field measurement campaign are available at the 4TU Centre for Research Data: https://doi.org/10.4121/collection:seawad, and tracer data are available here: https://doi.org/10.4121/15057378.

References

Allison, M.A., Yuill, B.T., Meselhe, E.A., Marsh, J.K., Kolker, A.S., Ameen, A.D., 2017. Observational and numerical particle tracking to examine sediment dynamics in a Mississippi River delta diversion. Estuar. Coast Shelf Sci. 194, 97–108. https://doi.org/10.1016/j.ecss.2017.06.004.

Balouin, Y., Howa, H., Michel, D., 2001. Swash platform morphology in the ebb-tidal delta of the Barra Nova inlet, South Portugal. J. Coast Res. 784 (174), 784–791.

Baptist, M.J., Gerkema, T., van Prooijen, B.C., van Maren, D.S., van Regteren, M., Schulz, K., Colosimo, I., Vroom, J., van Kessel, T., Grasmeijer, B., Willemsen, P., Elschot, K., de Groot, A.V., Cleveringa, J., van Eekelen, E.M.M., Schuurman, F., de Lange, H.J., van Puijenbroek, M.E.B., 2019. Beneficial use of dredged sediment to enhance salt marsh development by applying a 'Mud Motor.'. Ecol. Eng. 127 (November 2018), 312–323. https://doi.org/10.1016/j.ecoleng.2018.11.019.

Beamsley, B.J., Black, K.P., Healy, T., 2001. Micro-scale pumped measurements of suspended sediment over a mixed sand/mud bed: profiles, grain sizes and sediment diffusivity. J. Coast Res. 34, 342–356.

Bishop, M.J., Peterson, C.H., Summerson, H.C., Lenihan, H.S., Grabowski, J.H., 2006. Deposition and long-shore transport of dredge spoils to nourish beaches: impacts on benthic infauna of an ebb-tidal delta. J. Coast Res. 22 (3), 530–546. https://doi.org/10.2112/03-0136.1.

Black, K.S., Athey, S., Wilson, P., Evans, D., 2007. The use of particle tracking in sediment transport studies: a review. Geol. Soc., Lond., Spl. Publ. 274 (1), 73–91. https://doi.org/10.1144/GSL.SP.2007.274.01.09.

Black, K.S., Poleykett, J., Uncles, R.J., Wright, M.R., 2017. Sediment transport: instrumentation and methodologies. In: Uncles, R.J., Mitchell, S. (Eds.), Estuarine and Coastal Hydrography and Sediment Transport. Cambridge University Press, pp. 261–289.

Blackley, M.W.L., Heathershaw, A.D., 1982. Wave and tidal-current sorting of sand on a wide surf-zone beach. Mar. Geol. 49 (3–4), 345–355. https://doi.org/10.1016/0025-3227(82)90048-2.

Blott, S.J., Pye, K., 2001. Gradistat: a grain size distribution and statistics package for the analysis of unconsolidated sediments. Earth Surf. Process. Landforms 26 (11), 1237–1248. https://doi.org/10.1002/esp.261.

Brakenhoff, L., Kleinhans, M., Ruessink, G., van der Vegt, M., 2020a. Spatio-temporal characteristics of small-scale wave–current ripples on the Ameland ebb-tidal delta. Earth Surf. Process. Landforms 45 (5), 1248–1261. https://doi.org/10.1002/esp.4802.

Brakenhoff, L., Schrijvershof, R., van der Werf, J., Grasmeijer, B., Ruessink, G., van der Vegt, M., 2020b. From ripples to large-scale sand transport: the effects of bedform-related roughness on hydrodynamics and sediment transport patterns in Delft3D. J. Mar. Sci. Eng. 8 (11), 1–25. https://doi.org/10.3390/jmse8110892.

Carrasco, A.R., Ferreira, Ó., Matias, A., Freire, P., Bertin, X., Dias, J.A., 2013. Sediment transport measurements with tracers in very low-energy beaches. Earth Surf. Process. Landforms 38 (6), 561–569. https://doi.org/10.1002/esp.3300.

Cheung, K.F., Gerritsen, F., Cleveringa, J., 2007. Morphodynamics and sand bypassing at Ameland inlet, The Netherlands. J. Coast Res. 231, 106–118. https://doi.org/10.2112/04-0403.1.

Ciavola, P., Dias, N., Ferreira, Ó., Taborda, R., Dias, J.M.A., 1998. Fluorescent sands for measurements of longshore transport rates: a case study from Praia de Faro in southern Portugal. Geo Mar. Lett. 18 (1), 49–57. https://doi.org/10.1007/s003670050051.

Ciavola, P., Grottoli, E., 2017. Tracers and coarse sediment. In: Finkl, C.W., Makowski, C. (Eds.), Encyclopedia of Coastal Science. Springer International Publishing AG 2017, pp. 1796–1803.

Clemens, K.E., Komar, P.D., 1988. Tracers of sand movement on the Oregon coast. Coast. Eng. 1988, 1338–1351.

Courtois, G., Monaco, A., 1969. Radioactive methods for the quantitative determination of coastal drift rate. Mar. Geol. 7 (3), 183–206. https://doi.org/10.1016/0025-3227(69)90008-5.

de Schipper, M.A., Ludka, B.C., Raubenheimer, B., Luijendijk, A.P., Schlacher, T.A., 2021. Beach nourishment has complex implications for the future of sandy shores. Nat. Rev. Earth Environ. https://doi.org/10.1038/s43017-020-00109-9.

De Wit, F., Tissier, M., Reniers, A.J.H.M., 2019. Characterizing wave shape evolution on an ebb-tidal shoal. J. Mar. Sci. Eng. 7 (10), 1–20. https://doi.org/10.3390/jmse7100367.

Dean, R.G., 2002. Beach Nourishment: Theory and Practice. World Scientific.

Defeo, O., McLachlan, A., Schoeman, D.S., Schlacher, T.A., Dugan, J., Jones, A., Lastra, M., Scapini, F., 2009. Threats to sandy beach ecosystems: a review. Estuar. Coast Shelf Sci. 81 (1), 1–12. https://doi.org/10.1016/j.ecss.2008.09.022.

Duane, D., James, W., 1980. Littoral transport in the surf zone elucidated by an Eulerian sediment tracer experiment. J. Sediment. Res. 50 (3), 929–942. https://doi.org/10.1306/212F7B26-2B24-11D7-8648000102C1865D.

Elias, E.P.L., Pearson, S.G., van der Spek, A., Pluis, S., 2021. Understanding meso-scale processes at mixed-energy tide-dominated tidal inlet; Ameland Inlet, the Netherlands. Ocean and Coastal Management (Dutch Coastal Futures). OCMA-S-21-00338. In this issue.

Elias, E.P.L., Stive, M.J.F., Bonekamp, H., Cleveringa, J., 2003. Tidal inlet dynamics in response to human intervention. Coast Eng. J. 45, 629–658. https://doi.org/10.1142/S0578563403000932, 04.

Elias, E.P.L., Van Der Spek, A.J.F., Pearson, S.G., Cleveringa, J., 2019. Understanding sediment bypassing processes through analysis of high- frequency observations of Ameland Inlet, The Netherlands. Mar. Geol. 415, 105956 https://doi.org/10.1016/j.margeo.2019.06.001 (May).

Fontolan, G., Pillon, S., Delli Quadri, F., Bezzi, A., 2007. Sediment storage at tidal inlets in northern Adriatic lagoons: ebb-tidal delta morphodynamics, conservation and sand use strategies. Estuar. Coast Shelf Sci. 75 (1–2), 261–277. https://doi.org/10.1016/j.ecss.2007.02.029.

Foster, G., Healy, T.R., Lange, W. P. De, 1994. Sediment budget and equilibrium beach profiles applied to renourishment of an ebb tidal delta adjacent beach, Mt. Maunganui, New Zealand. J. Coast Res. 10 (3), 564–575.

Foster, I.D.L., 2000. Tracers in Geomorphology. John Wiley & Sons Ltd.

Gallaway, E., Trenhaile, A.S., Cioppa, M.T., Hatfield, R.G., 2012. Magnetic mineral transport and sorting in the swash-zone: northern Lake Erie, Canada. Sedimentology 59 (6), 1718–1734. https://doi.org/10.1111/j.1365-3091.2012.01323.x.

Gray, H.J., Jain, M., Sawakuchi, A.O., Mahan, S.A., Tucker, G.E., 2019. Luminescence as a sediment tracer and provenance tool. Rev. Geophys. 57 (3), 987–1017. https://doi.org/10.1029/2019RG000646.

Green, M.O., Bell, R.G., Dolphin, T.J., Swales, A., 2000. Silt and sand transport in a deep tidal channel of a large estuary (Manukau Harbour, New Zealand). Mar. Geol. 163 (1–4), 217–240. https://doi.org/10.1016/S0025-3227(99)00102-4.

Guymer, I., Stovin, V., Gaskell, P., Maltby, P.L., Pearson, J., 2010. Predicting the deposition of highway-derived sediments in a receiving river reach. In: Proc. 17th IAHR-APD Congress.

Hanes, D.M., 1988. Intermittent sediment suspension and its implications to sand tracer dispersal in wave-dominated environments. Mar. Geol. 81 (1–4), 175–183. https://doi.org/10.1016/0025-3227(88)90024-2.

Hanley, M.E., Hoggart, S.P.G., Simmonds, D.J., Bichot, A., Colangelo, M.A., Bozzeda, F., Heurtefeux, H., Ondiviela, B., Ostrowski, R., Recio, M., Trude, R., Zawadzka-Kahlau, E., Thompson, R.C., 2014. Shifting sands? Coastal protection by sand banks, beaches and dunes. Coast. Eng. 87, 136–146. https://doi.org/10.1016/j.coastaleng.2013.10.020.

Hanson, H., Brampton, A., Capobianco, M., Dette, H.H.H., Hamm, L., Laustrup, C., Lachuga, A., Spanhoff, R., 2002. Beach nourishment projects, practices and objectives – a European overview. Coast. Eng. 47, 81–111, 0378.

Herrling, G., Winter, C., 2018. Tidal inlet sediment bypassing at mixed-energy barrier islands. Coast. Eng. 140 (October 2017), 342–354. https://doi.org/10.1016/j.coastaleng.2018.08.008.

Hicks, D.M., Hume, T.M., 1997. Determining sand volumes and bathymetric change on an ebb-tidal delta. J. Coast Res. 13 (2), 407–416.

Huisman, B.J.A., de Schipper, M.A., Ruessink, B.G., 2016. Sediment sorting at the Sand Motor at storm and annual time scales. Mar. Geol. 381, 209–226. https://doi.org/10.1016/j.margeo.2016.09.005.

Kato, S., Okabe, T., Aoki, Y., Kamohara, S., 2014. Field measurement of sand movement on river-mouth tidal flat using color sand tracing. Coast. Eng. Proc. 1 (34), 61. https://doi.org/10.9753/icce.v34.sediment.61.

Keyence Corporation, 2014. VHX-5000 Digital Microscope User's Manual. Keyence Corporation.

Khalfani, D., Boutiba, M., 2019. Longshore sediment transport rate estimation near harbor under low and high wave-energy conditions: fluorescent tracers experiment. J. Waterw. Port, Coast. Ocean Eng. 145 (4) https://doi.org/10.1061/(ASCE)WW.1943-5460.0000517, 04019015.

Komar, P.D., 1978. Relative quantities of suspension versus bed-load transport on beaches. SEPM J. Sediment. Res. 48 (3), 921–932. https://doi.org/10.1306/212f75a9-2b24-11d7-8648000102c1865d.

Kraus, N.C., 1985. Field experiments on vertical mixing of sand in the surf zone. J. Sediment. Petrol. 55 (1), 3–14. https://doi.org/10.1306/212F85E9-2B24-11D7-8648000102C1865D.

Kraus, N.C., Isobe, M., Igarashi, H., Sasaki, T., Horikawa, K., 1982. Field experiments on longshore sand transport in the surf zone. Coast. Eng. 1982, 969–988.

Le Roux, J.P., Rojas, E.M., 2007. Sediment transport patterns determined from grain size parameters: overview and state of the art. Sediment. Geol. 202 (3), 473–488. https://doi.org/10.1016/j.sedgeo.2007.03.014.

Lenstra, K.J.H., Pluis, S.R.P.M., Ridderinkhof, W., Ruessink, G., van der Vegt, M., 2019. Cyclic channel-shoal dynamics at the Ameland inlet: the impact on waves, tides, and sediment transport. Ocean Dynam. 69 (4), 409–425. https://doi.org/10.1007/s10236-019-01249-3.

Li, H., Beck, T.M., Moritz, H.R., Groth, K., Puckette, T., Marsh, J., 2019. Sediment tracer tracking and numerical modeling at coos bay inlet, Oregon. J. Coast Res. 35 (1), 4. https://doi.org/10.2112/jcoastres-d-17-00218.1.

Liu, G., Cai, F., Qi, H., Zhu, J., Lei, G., Cao, H., Zheng, J., 2019. A method to nourished beach stability assessment: the case of China. Ocean Coast Manag. 177 (178), 166–178. https://doi.org/10.1016/j.ocecoaman.2019.05.015.

Lodder, Q.J., Wang, Z.B., Elias, E.P.L., van der Spek, A.J.F., de Looff, H., Townend, I.H., 2019. Future response of the wadden sea tidal basins to relative sea-level rise-an aggregated modelling approach. Water 11 (10). https://doi.org/10.3390/w11102198.

MacDonald, N.J., Davies, M.H., 2007. Particle-based sediment transport modelling. Coast. Eng. 3 (October), 3117–3128.

Malvern Instruments Limited, 2017. Mastersizer 3000 User Manual. Malvern Instruments Limited.

Martin, R.L., Jerolmack, D.J., Schumer, R., 2012. The physical basis for anomalous diffusion in bed load transport. J. Geophys. Res.: Earth Surf. 117 (1), 1–18. https://doi.org/10.1029/2011JF002075.

McComb, P., Black, K.P., 2005. Detailed observations of littoral transport using artificial sediment tracer, in a high-energy, rocky reef and iron sand environment. J. Coast Res. 21 (2), 358–373. https://doi.org/10.2112/03-574.1.

McLachlan, A., 1996. Physical factors in benthic ecology: effects of changing sand particle size on beach fauna. Mar. Ecol. Prog. Ser. 131 (1–3), 205–217. https://doi.org/10.3354/meps131205.

Miller, I.M., Warrick, J.A., 2012. Measuring sediment transport and bed disturbance with tracers on a mixed beach. Mar. Geol. 299–302, 1–17. https://doi.org/10.1016/j.margeo.2012.01.002.

Moritz, H., Puckette, T., Marsh, J., Boudreau, R., Siipola, M., Ott, M., 2011. Utilizing sediment tracer studies to evaluate transport pathways at the mouth of the columbia river, USA. Proc. Coast. Sed. 2011, 1565–1579. http://www.worldscientific.com/doi/abs/10.1142/9789814355537_0118.

Nortek, A.S., 2005. Vector current meter. User Manual (300–100) (Rev. H).

Nortek, A.S., 2008. Aquadopp high resolution. User Manual (AHR00–0101–0508).

Oertel, G., 1972. Sediment transport of estuary entrance shoals and the formation of swash platforms. J. Sediment. Res. 42 (4), 858–863. https://doi.org/10.1306/74D72658-2B21-11D7-8648000102C1865D.

Oliveira, S., Moura, D., Horta, J., Nascimento, A., Gomes, A., Veiga-Pires, C., 2017. The morphosedimentary behaviour of a headland–beach system: quantifying sediment transport using fluorescent tracers. Mar. Geol. https://doi.org/10.1016/j.margeo.2017.02.010.

Pearson, S.G., Prooijen, B.C., Elias, E.P.L., Vitousek, S., Wang, Z.B., 2020. Sediment connectivity: a framework for analyzing coastal sediment transport pathways. J. Geophys. Res.: Earth Surf. 125 (10) https://doi.org/10.1029/2020JF005595.

Pearson, S.G., Verney, R., van Prooijen, B.C., Tran, D., Hendriks, E.C., Jacquet, M., Wang, Z.B., 2021. Characterizing the composition of sand and mud suspensions in coastal and estuarine environments using combined optical and acoustic measurements. J. Geophys. Res.: Oceans 36, e2021JC017354. https://doi.org/10.1029/2021JC017354.

Peterson, C.H., Bishop, M.J., D'Anna, L.M., Johnson, G.A., 2014. Multi-year persistence of beach habitat degradation from nourishment using coarse shelly sediments. Sci. Total Environ. 487 (1), 481–492. https://doi.org/10.1016/j.scitotenv.2014.04.046.

Poizot, E., Mear, Y., Biscara, L., 2008. Sediment Trend Analysis through the variation of granulometric parameters: a review of theories and applications. Earth Sci. Rev. 86 (1–4), 15–41. https://doi.org/10.1016/j.earscirev.2007.07.004.

Reimann, T., Notenboom, P.D., de Schipper, M.A., Wallinga, J., 2015. Testing for sufficient signal resetting during sediment transport using a polymineral multiple-signal luminescence approach. Quat. Geochronol. 25, 26–36. https://doi.org/10.1016/j.quageo.2014.09.002.

Reniers, A.J.H.M., de Wit, F.P., Tissier, M.F.S., Pearson, S.G., Brakenhoff, L.B., van der Vegt, M., Mol, J., van Prooijen, B.C., 2019. Wave-skewness and current-related ebb-tidal sediment transport: observations and modeling. Coast. Sed. 2019, 2018–2028. https://doi.org/10.1142/9789811204487_0174.

Ribeiro, M., Taborda, R., Duarte, J., Rodrigues, A., 2018. Grain-size selective longshore transport at a headland-bay beach : insights from a sediment tracer experiment Grain-size selective longshore transport at a headland-bay beach : insights from a sediment tracer experiment. 5.as Jornadas de Engenharia Hidrográfica (July).

Ridderinkhof, H., Zimmerman, J.T.F., 1992. Chaotic stirring in a tidal system. Science 258 (5085), 1107–1111. https://doi.org/10.1126/science.258.5085.1107.

Rijkswaterstaat, 1999. Sedimentatlas waddenzee. Rijkswaterstaat. https://publicwiki.deltares.nl/display/OET/Dataset+documentation+Sediment+atlas+wadden+sea.

Robin, N., Levoy, F., Monfort, O., 2009. Short term morphodynamics of an intertidal bar on megatidal ebb delta. Mar. Geol. 260 (1–4), 102–120. https://doi.org/10.1016/j.margeo.2009.02.006.

Silva, A., Taborda, R., Rodrigues, A., Duarte, J., Cascalho, J., 2007. Longshore drift estimation using fluorescent tracers: new insights from an experiment at Comporta Beach, Portugal. Mar. Geol. 240 (1–4), 137–150. https://doi.org/10.1016/j.margeo.2007.02.009.

Smith, S.J., Marsh, J., Puckette, T., 2007. Analysis of fluorescent sediment tracer for evaluating nearshore placement of dredged material. Proc. 18th World Dredg. Congr., World Organ. Dredg. Assoc. 44, 1345–1358, 0. https://www.westerndredging.org/phocadownload/ConferencePresentations/2007_WODA_Florida/Session8B-PhysicalAndNumericalModeling/3-Smith-Fluorescent Sediment Tracer Evaluating Nearshore Placement Dredged Material.pdf.

Son, C.S., Flemming, B.W., Bartholomä, A., 2011. Evidence for sediment recirculation on an ebb-tidal delta of the East Frisian barrier-island system, southern North Sea. Geo Mar. Lett. 31 (2), 87–100. https://doi.org/10.1007/s00367-010-0217-8.

Soulsby, R.L., 1997. Dynamics of Marine Sands: a Manual for Practical Applications. In Dynamics of Marine Sands: a Manual for Practical Applications. Thomas Telford.

Soulsby, R.L., Mead, C.T., Wild, B.R., Wood, M.J., 2011. Lagrangian model for simulating the dispersal of sand-sized particles in coastal waters. J. Waterw. Port, Coast. Ocean Eng. 137 (3), 123–131. https://doi.org/10.1061/(ASCE)WW.1943-5460.0000074.

Stive, M.J.F., de Schipper, M.A., Luijendijk, A.P., Ranasinghe, R., van Thiel de Vries, J., Aarninkhof, S.G.J., Gelder-Maas, C. van, de Vries, S., Henriquez, M., Marx, S., 2013. The Sand Engine: a solution for vulnerable deltas in the 21st century? Coast. Dynam. 2013, 1537–1546.

Sunamura, T., Kraus, N.C., 1984. Prediction of average mixing depth of sediment in the surf zone. Mar. Geol. 62 (1–2), 1–12. https://doi.org/10.1016/0025-3227(84)90051-3.

van de Kreeke, J., Hibma, A., 2005. Observations on silt and sand transport in the throat section of the Frisian Inlet. Coast. Eng. 52 (2), 159–175. https://doi.org/10.1016/j.coastaleng.2004.10.002.

van der Spek, A.J.F., 1996. Holocene depositional sequences in the Dutch Wadden Sea south of the island of Ameland. Meded. Rijks Geol. Dienst 57, 41–78.

van der Werf, J., Antolínez, J.A.Á., Brakenhoff, L., Gawehn, M., den Heijer, K., de Looff, H., Wilmink, R., van Maarsseveen, M., Meijer-Holzhauer, H., Mol, J.-W., Pearson, S.G., van Prooijen, B., Santinelli, G., Schipper, C., Tissier, M., Tonnon, P.K., de Vet, L., Vermaas, T., Wilmink, R.J.A., de Wit, F., 2019a. Datareport Kustgenese 2.0 (1220339–15-NaN-4).

van der Werf, J.J., de Vet, P.L.M., Boersema, M.P., Bouma, T.J., Nolte, A.J., Schrijvershof, R.A., Soissons, L.M., Stronkhorst, J., van Zanten, E., Ysebaert, T., 2019b. An integral approach to design the Roggenplaat intertidal shoal nourishment. Ocean Coast Manag. 172 (February), 30–40. https://doi.org/10.1016/j.ocecoaman.2019.01.023.

Van Prooijen, B.C., Tissier, M.F.S., De Wit, F.P., Pearson, S.G., Brakenhoff, L.B., Van Maarseveen, M.C.G., Van Der Vegt, M., Mol, J.W., Kok, F., Holzhauer, H., Van Der Werf, J.J., Vermaas, T., Gawehn, M., Grasmeijer, B., Elias, E.P.L., Tonnon, P.K., Santinelli, G., Antolínez, J.A.A., De Vet, P.L.M., De Looff, H., 2020. Measurements of hydrodynamics, sediment, morphology and benthos on Ameland ebb-tidal delta and lower shoreface. Earth Syst. Sci. Data 12 (4), 2775–2786. https://doi.org/10.5194/essd-12-2775-2020.

Veenstra, H.J., Winkelmolen, A.M., 1976. Size, shape and density sorting around two barrier islands along the north coast of Holland. Geol. Mijnbouw 55 (1–2), 87–104 file://tsn.tno.nl/Data/SV/sv-066092/Refworks/Veenstra & Winkelmolen (1976).pdf.

Vila-Concejo, A., Ferreira, Ó., Ciavola, P., Matias, A., Dias, J.M.A., 2004. Tracer studies on the updrift margin of a complex inlet system. Mar. Geol. 208 (1), 43–72. https://doi.org/10.1016/j.margeo.2004.04.020.

Vila-Concejo, A., Ferreira, Ó., Ciavola, P., Taborda, R., Dias, J.M.A., 2003. Quantitative and qualitative analyses of tracer data: straight beaches, inlets and harbours. Proc. Coast. Sed.

Wang, Y., Yu, Q., Jiao, J., Tonnon, P.K., Wang, Z.B., Gao, S., 2016. Coupling bedform roughness and sediment grain-size sorting in modelling of tidal inlet incision. Mar. Geol. 381 (September), 128–141. https://doi.org/10.1016/j.margeo.2016.09.004.

Wang, Z.B., Elias, E.P.L., van der Spek, A.J.F., Lodder, Q.J., 2018. Sediment budget and morphological development of the Dutch Wadden Sea: impact of accelerated sea-level rise and subsidence until 2100. Neth. J. Geosci. 97, 183–214. https://doi.org/10.1017/njg.2018.8, 03.

Wang, Z.B., Van Maren, D.S., Ding, P.X., Yang, S.L., van Prooijen, B.C., de Vet, P.L.M., Winterwerp, J.C., De Vriend, H.J., Stive, M.J.F., He, Q., 2015. Human impacts on morphodynamic thresholds in estuarine systems. Continent. Shelf Res. 111, 174–183. https://doi.org/10.1016/j.csr.2015.08.009.

White, T.E., 1998. Status of measurement techniques for coastal sediment transport. Coast. Eng. 35 (1–2), 17–45. https://doi.org/10.1016/S0378-3839(98)00033-7.

Wilson, G.W., 2018. Anomalous diffusion of sand tracer particles under waves. J. Geophys. Res.: Earth Surf. 123 (11), 3055–3068. https://doi.org/10.1029/2018JF004780.